Theor Chem Account (2008) 120:385–393
DOI 10.1007/s00214-008-0416-9

REGULAR ARTICLE

MP2 Study of synergistic effects between X–H/π (X = C,N,O) and π–π interactions

David Quiñonero · Antonio Frontera · Daniel Escudero · Pablo Ballester · Antoni Costa · Pere M. Deyà

Received: 24 September 2007 / Accepted: 4 February 2008 / Published online: 19 February 2008

Abstract In this manuscript we report high level ab initio calculations [RI-MP2(full)/aug-cc-pVDZ] and experimental evidence that demonstrate that important synergistic effects between two relevant non covalent interactions that are omnipresent in biological systems, i.e., π–π and X–H/π interactions (X = C,N,O), occur when the interactions coexist in the same complex. In particular, we study how the π–π interaction influences the X–H/π interaction and vice versa by computing the genuine non additivity energies of the ternary X–H/π–π complexes.

Keywords Non covalent interactions · Synergistic effects · Stacking · C–H/π interaction

1 Introduction

Non covalent interactions play a key role in many areas of modern chemistry, especially in the field of supramolecular chemistry and molecular recognition [1]. In particular, interactions involving aromatic rings are key processes in both chemical and biological recognition and they have been recently reviewed by Meyer et al. [2]. For instance, cation-π interactions [3–8] are supposed to be an important factor to the ion selectivity in potassium channels [9,10], they are also important for the binding of acetylcholine to the active site of the enzyme acetylcholine esterase [11], and, recently, their importance has been demonstrated in neurotransmitter receptors [12]. In addition, attractive interactions between π systems are very important forces that govern molecular recognition and influence structures of proteins, DNA and solid materials. The C–H/π interaction [13] can be defined as the attraction between the C–H bond and the π system [14] and has recently gained attention in the consideration of a variety of molecular phenomena. Despite being the weakest among the hydrogen bonds, it has been found in a variety of substances to play important roles in their physical, chemical and biological properties [15–18]. While the enthalpy for a "conventional hydrogen bond" is within the range of 3–7 kcal/mol, the one for a one-pair C–H/π interaction is presumed to be less than 1 kcal/mol [19]. The total energy of the interaction is increased by organizing CHs or π-groups into favorable structures. This point is important in understanding the role of weak interactions. Hunter's group [20] has used an amide macrocycle with a highly preorganized cavity containing both polar and non-polar recognition sites to form stable complexes with cyclic peptides in water via hydrogen-bonds, N–H/π and C–H/π interactions. Complexes of π-electron systems with standard hydrogen-bond donors have been examined and identified as a particular type of hydrogen bond interaction [21–24]. The stabilization energy in these complexes stems from both electrostatic (50–70% of the interaction energy depending on the donor) and dispersion forces [25–27]. The CH group can be considered as a weak hydrogen bond donor in complexes between alkyl or aryl groups with aromatic rings [28,29]. On the basis of theoretical calculations, some of these interactions have been identified as improper hydrogen bonds [30–32]. The interaction is weak for benzene complexes [19] and slightly stronger for larger aromatic rings [33]. Lastly, π–π interactions [34] are weak

Contribution to the Nino Russo Special Issue.

D. Quiñonero · A. Frontera (✉) · D. Escudero · A. Costa · P. M. Deyà
Department of Chemistry, Universitat de les Illes Balears, Crta. de Valldemossa km 7.5, 07122 Palma de Mallorca, Spain
e-mail: toni.frontera@uib.es

P. Ballester
ICREA and Institute of Chemical Research of Catalonia (ICIQ), Avinguda Països Catalans 16, 43007 Tarragona, Spain

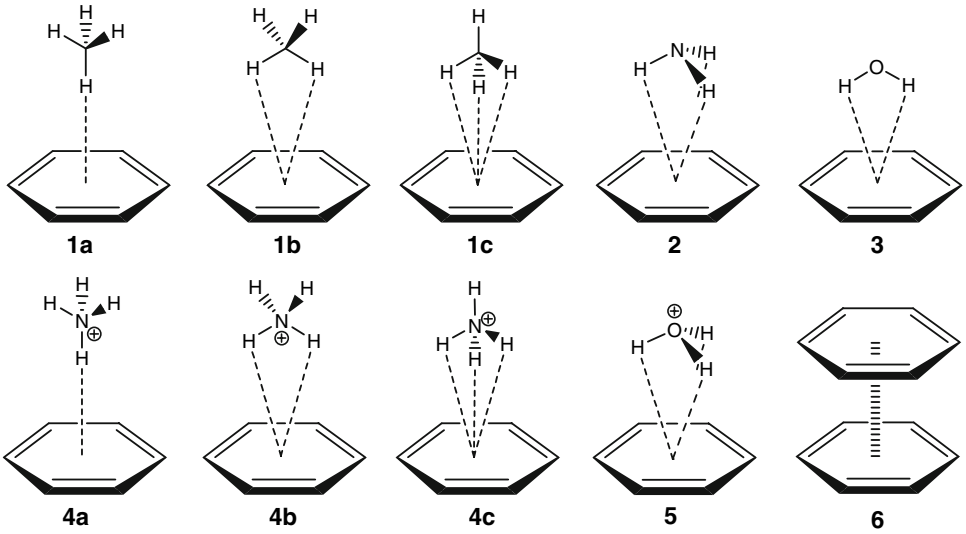

Fig. 1 Schematic representation of binary complexes **1–6**

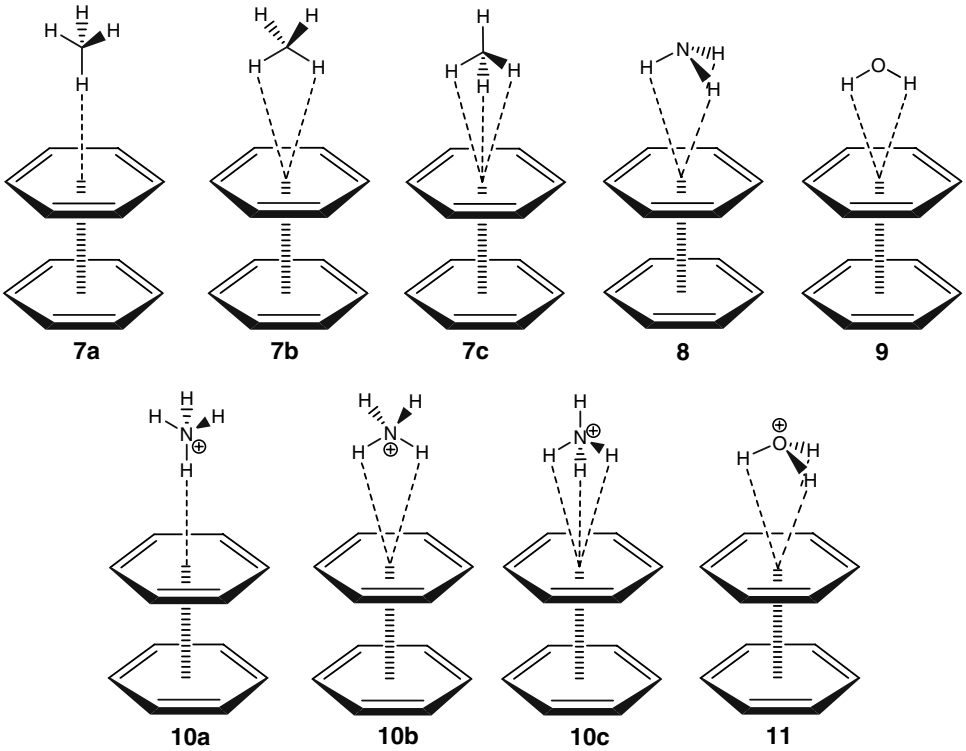

Fig. 2 Schematic representation of ternary complexes **7–11**

non covalent forces that play an essential role in the folding of proteins [35], in the structure of DNA as well as in its interactions with small molecules [36,37]. They are widely used in supramolecular chemistry and are very important binding forces that determine the packing of organic molecules in crystals. They are also used in crystal engineering for the design of functional materials [38]. Moreover, non covalent nanostructures, such as polymeric networks [39], dendrimers [40], "onions" [41], and "peapods" [42] have been successfully constructed using aromatic π–π stacking interactions between the surface of fullerenes and different kinds of receptors. These concave–convex π–π stacking interactions have been recently reviewed [43]. The physical nature of the π–π interaction has been extensively studied by Hobza's group [44–51].

In this manuscript, we study how the π–π and the X–H/π interactions influence each other. To achieve that, we have optimized the complexes present in Figs. 1 and 2 and computed their interaction energies. We have computed the 1:1 complexes present in Fig. 1 and the ternary 1:1:1 X–H/π–π complexes present in Fig. 2, in order to study the interplay between the π–π and X–H/π interactions. We have used

the Bader's theory of "atoms-in-molecules" (AIM) [52,53], which has been widely used to characterize a great variety of interactions [54–56], to analyze cooperative effects in the complexes. We have found that the X–H/π interaction reinforces the π–π interaction and vice versa to a minor extend.

2 Computational methods

The geometries of all complexes studied in this work were fully optimized using the resolution of the identity MP2 (RI-MP2) level and the aug-cc-pVDZ basis set. The RI-MP2 (full) calculations were done using the program TURBOMOLE version 5.7 [57]. The RI-MP2 method [58,59] applied to the study of interactions involving aromatic rings is considerably faster than the MP2 and the interaction energies and equilibrium distances are almost identical for both methods [60,61]. It has been recently published [62] that the MP2/aug-cc-pVDZ level of theory gives comparable results to the CCSD(T) method using the basis set limit approximation for CH_4-benzene complexes. This is probably due to a fortuitous error cancellation [62]. In addition, although it is well-known [63] that the MP2 method overestimates the π–π interaction, the aug-cc-pVDZ basis set gives better results for the description of the π–π interaction in the sandwich benzene dimer than larger basis sets, in comparison with the CCSD(T)/aug-cc-VQZ level of theory [64]. The binding energies were calculated with correction for the basis set superposition error (BSSE) by using the counterpoise technique [65]. The optimization of the complexes has been performed imposing C_{nv} symmetry, where n is two in complexes **1b**, **3**, **4b**, **7b**, **9** and **10b**; and n is three in the rest of complexes, except the optimization of complex **6**, which has been performed imposing D_{6h} symmetry. The topological analysis of the electron charge density performed for the complexes **1**–**11** was determined using Bader's theory of "atoms-in-molecules". The electronic density analysis was performed using the AIM2000 program [66] by means of the MP2/aug-cc-pVDZ//RI-MP2(full)/aug-cc-pVDZ wavefunction. This methodology has been found useful for analyzing and relating the AIM properties at the critical points with the strength of the ion–π interaction [67].

The physical nature of the interaction has been studied using the Molecular Interaction Potential with polarization (MIPp) [68] methodology. The MIPp is a convenient tool for predicting binding properties. It has been successfully used for rationalizing molecular interactions such us hydrogen bonding and ion–π interactions and for predicting molecular reactivity [69–71]. MIPp is an improved generalization of the MEP where three terms contribute to the interaction energy, (i) an electrostatic term identical to the MEP [72], (ii) a classical dispersion–repulsion term, and (iii) a polarization term derived from perturbational theory [73]. Calculation of the MIPp of benzene and benzene dimer **6** was performed using the HF wavefunction of the aromatic rings by means of the MOPETE-98 program [74]. Calculation of MIPp using the MP2 wavefunction are not available [74].

3 Results and discussion

In Table 1, we summarize the binding energies and equilibrium distances obtained for 1:1 complexes **1**–**6**. As expected, the X–H/π complexes of benzene (BEN) with neutral species give very modest binding energies and the complexes with charged species **4a**–**c** and **5** give more favorable binding energies. The most favorable orientation for the interaction of CH_4 with BEN is **1a**, where only one hydrogen atom of methane is pointing to the center of the ring. For this complex the interaction energy is −1.5 kcal/mol, in good agreement with the value obtained at the CCSD(T)/limit level of theory, i.e. −1.4 kcal/mol [62]. Moreover, the binding energy and equilibrium distance obtained for **1a** at the RI-MP2 and MP2/aug-cc-pVDZ levels of theory are identical, giving reliability to the RI approximation. The other two orientations **1b** and **1c** have similar binding energies. The interaction energy of the complex of NH_3 with BEN (**2**) is comparable to **1c** indicating that the N–H/π interaction is comparable to the C–H/π interaction, when the binding mode is C_{3v} using three hydrogen atoms. The O–H/π interaction is energetically more favorable than the N–H/π, as deduced by the interaction energy computed for complex **3** (−2.6 kcal/mol). This trend is in agreement with previous theoretical [75] and experimental [76,77] results. The binding energies of charged complexes **4** and **5** are considerably more favorable than neutral since for former complexes there are important electrostatic effects (charge-quadrupole

Table 1 Interaction energies without (E, kcal/mol) and with (E_{CP}, kcal mol) the BSSE correction and equilibrium distances (R_e, Å) computed at the RI-MP2(full)/aug-cc-pVDZ level of theory for **1**–**6**

Compound	E	E_{CP}	R_e
1a	−3.6	−1.5	3.69
1b	−3.3	−1.2	3.45
1c	−3.1	−1.1	3.40
2	−3.2	−1.3	3.36
3	−4.9	−2.6	3.17
4a	−21.7	−17.7	2.94
4b	−22.4	−18.6	2.86
4c	−20.5	−17.1	2.88
5	−27.5	−23.5	2.72
6	−6.3	−2.8	3.61

Table 2 Interaction (E_{CP}, kcal/mol) energies with the BSSE correction, non-additivity energies ($E - E_A$, kcal/mol) and equilibrium distances (R_e and R_s, Å) computed at the RI-MP2(full)/aug-cc-pVDZ level of theory for complexes **7–11**

Compound	E	E_{CP}	$E - E_A$	R_s^a	R_e
7a	−10.6	−3.7	−0.3	3.50	3.52
7b	−10.2	−3.7	−0.4	3.51	3.45
7c	−10.0	−3.5	−0.4	3.51	3.40
8	−10.2	−4.0	−0.6	3.51	3.36
9	−12.1	−5.5	−0.5	3.51	3.17
10a	−32.1	−23.4	−1.5	3.48	2.94
10b	−33.1	−24.3	−2.2	3.44	2.84
10c	−31.0	−22.7	−2.1	3.44	2.86
11	−39.3	−30.0	−4.9	3.40	2.70

[a] R_s stands for the stacking distance and R_e for the heteroatom to ring centroid distance

interactions). Parallel to the behavior of the neutral complexes, the O^+–H/π interaction is more favorable than the N^+–H/π interaction. The most favorable orientation for the NH_4^+ and BEN is **4b** (C_{2v}), which is in agreement with a previously reported theoretical study [78].

In order to analyze the influence of X–H/π interactions on the π–π interaction we have computed the ternary complexes **7–11** (see Figure 2). The geometric and energetic results obtained for these complexes are summarized in Table 2. Some interesting points can be extracted from the results. First, the equilibrium distance of the π–π stacking interaction in the ternary complexes **7–11** shortens when compared to 1:1 complex **6**, indicating that the presence of the X–H/π interaction strengthens the π–π interaction. In addition, in the ternary complexes where the interacting hydrogen atom belongs to a charged species (**10a–c** and **11**), the equilibrium distance (R_s) of the π–π interaction shortens more than in neutral complexes, indicating that the π–π interaction is more reinforced in charged than in neutral complexes. Moreover, in the ternary complexes the equilibrium distance (R_e) of the X–H/π interaction is poorly sensitive to the presence of the π–π interaction. In neutral complexes, this distance is almost unaltered in comparison with the binary complexes apart from complex **7a**, where the equilibrium distance R_e shortens 0.15 Å with respect to the 1:1 complex **1a**. In charged complexes, there is a very modest shortening of the R_e distances (0.02 Å). This geometrical analysis indicates that the coexistence of both interactions in the same complex mainly strengthens the π–π interaction and the X–H/π interaction is either unaltered or slightly strengthened. Second, we have included in the table what we entitle genuine non-additivity energy ($E - E_A$). It is the difference between the binding energy of the ternary 1:1:1 complex and the binding energy of the sum of all pair interaction energies (denoted as E_A). For instance, in complex **7a** [$CH_4 \cdots (R_e) \cdots BEN \cdots (R_s) \cdots BEN$] we have computed the non-additivity energy by subtracting the sum of three pair interaction energies: (i) $CH_4 \cdots (R_e) \cdots$ BEN, (ii) $CH_4 \cdots (R_e + R_s) \cdots$ BEN and (iii) BEN $\cdots (R_s) \cdots$ BEN from the binding energy of **14**. This value gives valuable information regarding the interplay between both non covalent interactions present in the ternary complexes. It is worth mentioning that this term is negative in all complexes, indicating that there is a favorable interplay between both non covalent interactions. For neutral complexes this term is very small (less than 1 kcal/mol), but not negligible taking into account that the interaction energies of the complexes are small, ranging from −5.5 to −3.7 kcal/mol. These results indicate an small cooperativity of both interactions in terms of energetic parameters. In charged complexes, the $E - E_A$ values are higher in magnitude, indicating that the interplay between both non covalent interactions is more important in these systems. The energetic analysis of synergistic effects in the complexes is in agreement with the geometrical results.

The AIM analysis is summarized in Table 3 and it gives some helpful information regarding the strength of the non-covalent interactions involved in the complexes. It has been demonstrated that the value of the electron charge density at the cage critical point (CP) that it is generated upon complexation in systems involving aromatic rings can be used as a measure of the bond order [56,60,61]. In Fig. 3 we show the distribution of CPs in complexes **7a**, **8** and **10b**, as representative examples of X–H/π–π complexes with C_{3v} (one H atom pointing to the ring centroid), C_{3v} and C_{2v} symmetries, respectively. In all ternary complexes and the binary complex **6**, six bond CPs, six ring CPs and one cage CP describe the π–π interaction. The X–H/π interaction description depends upon the symmetry of the complex. In C_{3v} complexes **1a** and **4a** the interaction is described by six bond CPs, six ring CPs and one cage CP. The bond CPs connect the hydrogen atom with the carbon atoms of the ring, the ring CPs connect the hydrogen atom with the middle of the C–C bonds of the aromatic ring and the cage CP connects the hydrogen atom with the center of the ring along the main symmetry axis. In C_{3v} complexes **1c**, **2**, **4c**, **5**, **7c**, **8**, **10c** and **11**, the X–H/π interaction is described by three bond CPs, three ring CPs and one cage CP. The bond CPs connect three hydrogen atoms with three alternated carbon atoms of the ring, the ring CPs connect the heteroatom with the other three carbon atoms of the aromatic ring and the cage CP connects the heteroatom with the center of the ring along the main symmetry axis. In C_{2v} complexes, the X–H/π interaction is described by two bond CPs, two ring CPs and one cage CP. The bond CPs connect two hydrogen atoms with two carbon atoms of the ring, the ring CPs connect the heteroatom with the middle of two opposite C–C bonds of the aromatic ring and the cage

Table 3 Electron charge density (ρ, a.u.) computed at the cage critical points for complexes **1–11** and the variation upon formation of the ternary complexes **7–11** with respect to the related 1:1 complexes **1–6**. Variation of the R_e and R_s equilibrium distances of the ternary complexes **7–11** with respect to the related 1:1 complexes **1–6** (ΔR_e and ΔR_s)

Compound	$10^2 x\rho$ (3, +3), X–H/$-\pi$ $10^2 x\rho$ (3, +3), π–π	$10^4 x\Delta\rho$ (3, +3), X–H/$-\pi$ $10^4 x\Delta\rho$ (3,+3), π–π	ΔR_e ΔR_s
1a	0.4459	–	–
1b	0.3359	–	–
1c	0.2993	–	–
2	0.3930	–	–
3	0.4644	–	–
4a	1.1307	–	–
4b	0.7190	–	–
4c	0.6067	–	–
5	0.8184	–	–
6	0.1730	–	–
7a	0.5753	13.04	*−0.17*
	0.1906	*1.76*	*−0.11*
7b	0.3386	0.27	0.00
	0.1879	*1.48*	*−0.10*
7c	0.3000	0.07	0.00
	0.1896	*1.66*	*−0.10*
8	0.3943	0.13	0.00
	0.1867	*1.37*	*−0.10*
9	0.4708	0.64	0.00
	0.1879	*1.49*	*−0.10*
10a	1.1405	0.98	0.00
	0.1929	*1.99*	*−0.13*
10b	0.7526	3.56	0.02
	0.2060	*3.30*	*−0.17*
10c	0.6326	2.95	0.02
	0.2027	*2.97*	*−0.17*
11	0.8517	3.33	0.02
	0.2162	*4.32*	*−0.21*

The values in italics of ρ correspond to the cage (3, +3) CP located between the aromatic rings along the main symmetry axis and the variation of the stacking distance in ternary complexes (ΔR_s)

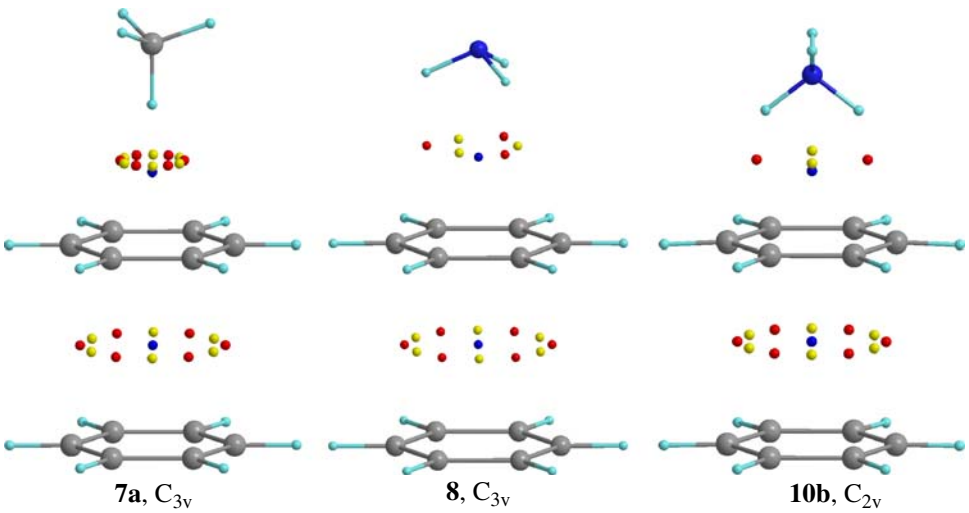

Fig. 3 Schematic representation of the location of bond (*red*), ring (*yellow*) and cage (*blue*) CPs in complexes **7a**, **8** and **10b**

Table 4 Contributions to the total interaction energy (kcal/mol) computed using MIPp of benzene (BEN) and its dimer **6** interacting with H^{n+} ($n = 0.1$, 0.2, 0.4 and 0.6) at the minimum along the C_6 axis

Charge (e)	E_e		E_p		E_{vw}		E_t	
	BEN	**6**	BEN	**6**	BEN	**6**	BEN	**6**
0.1	−1.44	−1.77	−0.13	−0.14	−0.39	−0.40	−1.96	−2.31
0.2	−3.02	−3.71	−0.56	−0.63	−0.31	−0.21	−3.89	−4.55
0.4	−6.33	−7.76	−2.48	−2.81	0.13	0.14	−8.68	−10.43
0.6	−10.29	−12.59	−6.22	−7.84	0.71	1.76	−15.80	−18.68

CP connects the heteroatom with the center of the ring along the main symmetry axis (see Fig. 3). In Table 3 we summarize the values of the electron charge density (ρ) computed at the cage critical points for complexes **1**–**11**. We also summarize the variation of these values in the ternary complexes **7**–**11** with respect to the binary complexes **1**–**6**. These values give information about the strengthening of the non-covalent interaction involved in the complexes. First, it is worth mentioning that the value of the charge density computed at the cage CPs is greater in the ternary complexes than in the binary complexes, in agreement with the computed non additivity energies and geometric features of the complexes. Second, these results confirm that the concurrent formation of π–π and X–H/π interactions has a synergistic effect that is related to the increase in the values of ρ at the cage CPs and, consequently, with the reinforcement of the non covalent interactions. In Table 3 we also include the variation of R_e and R_s in the ternary complexes with respect to the binary complexes (ΔR_e and ΔR_s). It can be observed that the values are always negative for the R_s distance (π–π stacking), in agreement with the variation of the charge density at the cage CP that describe the π–π interaction (values in italics in Table 3). The variation of the charge density at the cage CP that describes the X–H/π interaction indicates that the reinforcement of this interaction is, in general, modest, with the exception of complex **7a**, in agreement with the values of ΔR_e. It should be mentioned that the values of ΔR_e and $\Delta\rho$ computed for **7a** are considerable greater than the values computed for similar complexes **7b**, **c**, whilst the non-additivity energies are similar for all **7a**–**c** complexes (see Table 2). The higher value of ΔR_e can be explained considering the geometric features of complex **1a**, where the distance from the carbon atom of the interacting methane to the ring centroid is much longer than in the other methane–benzene complexes **1b**, **c**. This issue allows a major shortening of the equilibrium distance in **7a**. Moreover, a likely explanation for the important $\Delta\rho$ value in **7a**, which agrees with the ΔR_e value, is that the charge density at the cage critical point is more sensitive to the equilibrium distance than to the binding energy of the complex. It has been reported that the ρ value is linear dependent upon the binding energy [79–82] and it is exponential dependent upon the equilibrium distance [83–85].

We have used the MIPp partition scheme to analyze the physical nature of the C–H/π interaction involved in the complexes and to understand the bonding mechanism and the synergistic effects. We have computed the MIPp of benzene and the dimer of benzene **6** interacting with H in order to study the C–H/π interaction in the absence and presence of π–π stacking (see Table 4). We have performed the calculations assigning to the H several charges in order to simulate a variety of situations, i.e., the hydrogen atom bonded to a neutral (CH_4, H_2O, NH_3) or charged atom (NH_4^+ and H_3O^+). When the interacting hydrogen has a low charge (0.1–0.2 e) the interaction is basically dominated by electrostatic effects (E_e), since the polarization (E_p) and dispersion-repulsion contributions (E_{vw}) are small. At higher charge values (0.4–0.6 e) the E_p term increases but the E_e dominates the interaction (65–70%). The MIPp analysis indicates that the physical nature of the synergistic effect is electrostatic. The benzene dimer has higher interaction energies than benzene and it is due to the electrostatic term for the all range of charges assigned to the hydrogen. The MIPp results are in agreement with the complexation and non additivity energies of Tables 1 and 2.

As stated in the introduction the C–H/π and π–π interactions are of pivotal importance in biological systems, where these interactions are omnipresent. In the theoretical study discussed above, we have demonstrated that there is an interesting interplay between both interactions and that their coexistence has a positive synergistic effect. It is probable that both interactions may coexist in relevant biological processes and participate in the binding mechanism of a substrate at the binding site of an enzyme. We have explored the Protein Data Bank (PDB) database in order to find examples where an aromatic ligand interacts with the active center of a protein using both interactions simultaneously. To illustrate this issue, we have selected three examples retrieved from the PDB where the coexistence of both interactions is evident and relevant. The first example is represented in Fig. 4 and the PDB code is 1eve [86]. The substrate is an acetylcholinesterase (AChE) inhibitor that is being used for symptomatic treatment of Alzheimer's disease. E2020, marketed as Aricept®, is a member of a family of *N*-benzylpiperidine-based AChE inhibitors. The experimental three-dimensional

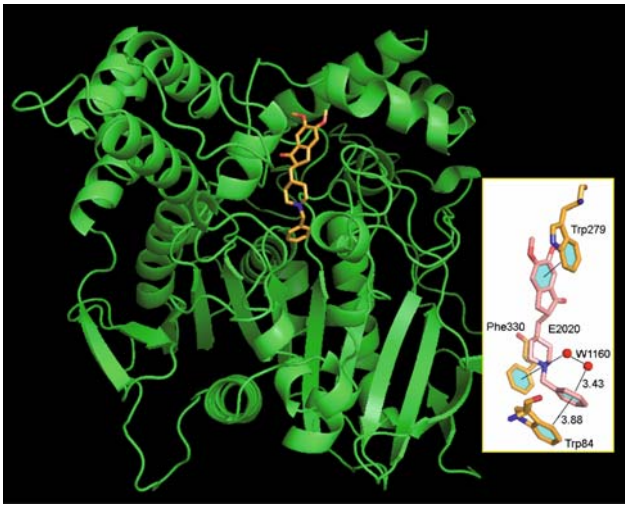

Fig. 4 Structure of the complex between the anti-Alzheimer drug E2020 (represented by sticks) and acetylcholinesterase (represented by a ribbon diagram of the polypeptide backbone). The interactions of E2020 and acetylcholinesterase involving aromatic rings at the active site of the enzyme are highlighted at the right side of the figure. Distances in Å

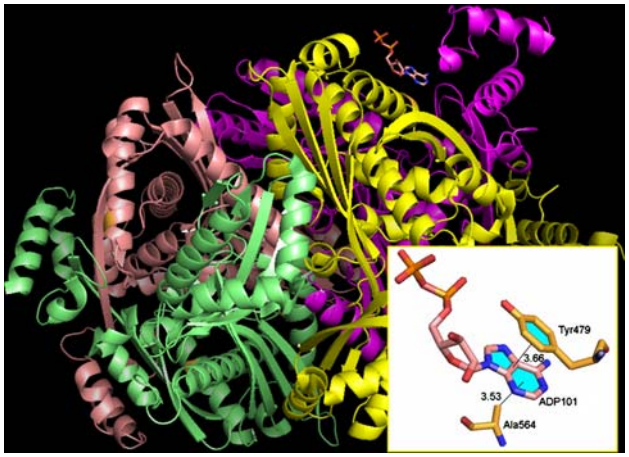

Fig. 5 Structure of the complex between the ADP cofactor (represented by sticks) and HMG-CoA reductase (represented by a ribbon diagram of the polypeptide backbone). The interactions of ADP and the enzyme involving aromatic rings are highlighted at the right side of the figure. Distances in Å

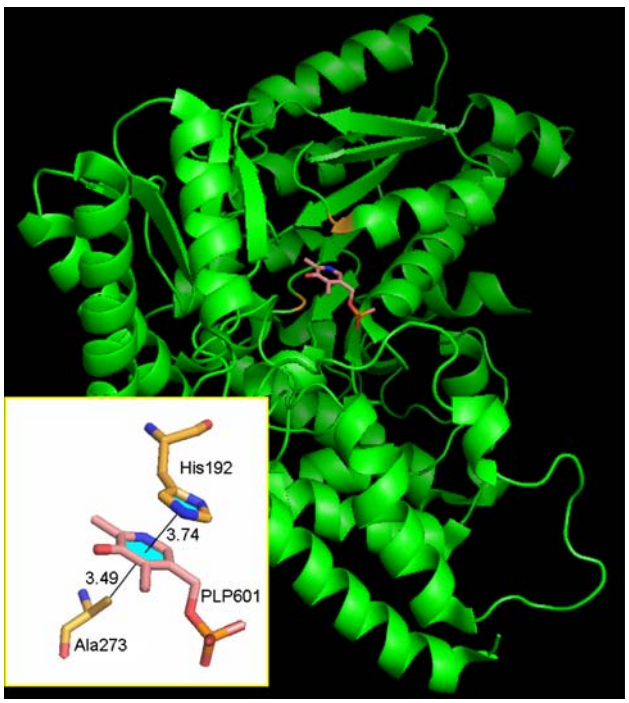

Fig. 6 Structure of the complex between the pyridoxal-5′-phosphate (PLP) cofactor (represented by sticks) and DOPA-decarboxylase (represented by a ribbon diagram of the polypeptide backbone). The interactions of PLP and the enzyme involving aromatic rings are highlighted at the left side of the figure. Distances in Å

structure shown in Fig. 4 corresponds to *Torpedo californica* AChE (TcAChE) complex with E2020. The high affinity and selectivity of E2020 was justified by the original authors arguing specific interactions via aromatic stacking with several amino acids of the active site. These interactions are highlighted in Fig. 4. In one of them, there is an O–H/π interaction between a water molecule and the phenyl ring of E2020. Concurrently, this phenyl ring is establishing a π–π stacking interaction with the Trp84, giving rise to an O–H/π–π interaction.

The second example retrieved from the PDB (code 1hwi [87]) is shown in Fig. 5. It is a complex between HMG-CoA (3-hydroxy-3-methylglutaryl-coenzymeA) reductase (HMGR) and its inhibitor fluvastin. HMGR catalyzes the committed step in cholesterol biosynthesis. Fluvastin in the nanomolar range effectively lower serum cholesterol levels and are widely prescribed in the treatment of hypercholesterolemia. In the illustration of Fig. 5 we represent the interaction of the cofactor with the enzyme (*Homo sapiens* HMGR, catalytic portion). The adenosine π-system is forming a π–π stacking interaction with the Tyr479 of one chain of the enzyme and it is participating in a C–H/π interaction with the Ala564 of another chain of the enzyme.

The last example that we have selected to exemplify the coexistence of both interactions in biological systems is represented in Fig. 6. The PDB code is 1js3 [88]. The enzyme is L-3,4-dihydroxyphenylalanine (L-DOPA) decarboxylase (DDC). This enzyme is responsible for the synthesis of dopamine and serotonin via decarboxylation of DOPA. DDC has been implicated in a number of clinic disorders such as hypertension and Parkinson's disease. Inhibitors of DDC are currently used to treat them. DDC is a tightly associated α_2-dimer (only one monomer is shown in Fig. 6) and it belongs to the family of pyridoxal-5′-phosphate (PLP)-dependent enzymes. In the figure, we show the complex of DDC with the cofactor PLP, which is illustrated in sticks

representation. In the left part of the figure the interactions of PLP with the enzyme are exposed. It can be easily appreciated that the aromatic ring of the PLP is participating in a C–H/π interaction with the residue Ala273. In addition, the aromatic ring is also participating in a π–π stacking interaction with the residue His192 of the enzyme. It is interesting to note that in this case the aromatic aminoacid that participates in the π–π interaction is histidine by means of the imidazole ring.

4 Conclusion

In summary, the results reported in this manuscript stress the importance of non covalent interactions involving aromatic systems and the interplay among them, that can lead to synergistic effects. They are modest in magnitude for neutral molecules, nevertheless its contribution to the total interaction energy is important. The synergistic effects have been successfully studied examining energetic and geometrical parameters of the complexes and by means of the analysis of the electron charge density using the Bader's theory of "atoms-in-molecules" at the cage CPs that appear upon complexation. Due to the presence of a great number of C–H/π and π–π interactions in biological systems, cooperativity effects between non covalent interactions can be important and might help to understand some biological processes where the interplay between both interactions exist. Finally, we have explored the PDB and we have found several examples that demonstrate that both interactions coexist in the binding of substrates and cofactors to the active center of several important enzymes.

Acknowledgments We thank the DGICYT of Spain (projects CTQ2005-08989-01 and CTQ2005-08989-02) for financial support. We thank the Govern Balear project PROGECIB-33A for financial support. We thank the Centre de Supercomputació de Catalunya (CESCA) for computational facilities. D. Q. thanks the MCyT for a "Juan de la Cierva" contract. D. E. thanks the MEC for a fellowship.

References

1. Hunter CA, Sanders JKM (1990) J Am Chem Soc 112:5525
2. Meyer EA, Castellano RK, Diederich F (2003) Angew Chem Int Ed 42:1210
3. Ma JC, Dougherty DA (1997) Chem Rev 97:1303
4. Gallivan JP, Dougherty DA (1999) Proc Natl Acad Sci USA 96:9459
5. Gokel GW, Wall SLD, Meadows ES (2000) Eur J Org Chem 2967
6. Gokel GW, Barbour LJ, Wall SLD, Meadows ES (2001) Coord Chem Rev 222:127
7. Gokel GW, Barbour LJ, Ferdani R, Hu J (2002) Acc Chem Res 35:878
8. Hunter CA, Singh J, Thorton JM (1991) J Mol Biol 218:837
9. Kumpf RA, Dougherty DA (1993) Science 261:1708
10. Heginbotham L, Lu Z, Abramson T, Mackinnon R (1994) Biophys J 66:1061
11. Dougherty DA (1996) Science 271:163
12. Lummis SCR, Beene DL, Harrison NJ, Lester HA, Dougherty DA (2005) Chem Biol 12:993
13. Kodama Y, Nishihata K, Nishio M, Nakagawa N (1977) Tetrahedron Lett 18:2105
14. Nishio M, Hirota M, Umezawa Y (1998) The C-H/π interaction evidence, nature, and consequences. Wiley-VCH, Inc, New York
15. Quiocho FA, Vyas NK (1984) Nature 310:381
16. Vyas NK, Vyas MN, Quiocho FA (1987) Nature 327:635
17. Umezawa Y, Tsuboyama S, Takahashi H, Uzawa J, Nishio M (1999) Tetrahedron 55:10047
18. Amabilino DB, Ashton PR, Balzani V, Boyd SE, Credi A, Lee JY, Menzer S, Stoddart JF, Venturi M, Williams DJ (1998) J Am Chem Soc 120:4295
19. Tsuzuki S, Honda K, Uchimaru T, Mikami M, Tanabe K (2000) J Am Chem Soc 122:3746
20. Allot C, Bernard PL, Hunter CA, Rotger C, Thomas JA (1998) Chemm Commun 2449
21. Oki M, Iwamura H (1959) Bull Chem Soc Jpn 32:955
22. Perutz MF, Fermi G, Abraham DJ, Poyart C, Bursaux E (1986) J Am Chem Soc 108:1064
23. Burley SK, Petsko GA (1986) FEBS Lett 203:139
24. Suzuki S, Green PG, Bumgarner RE, Dasgupta S, Goddard WA III, Blake GA (1992) Science 257:942
25. Tsuzuki S, Honda K, Uchimaru T, Mikami M, Tanabe K (2000) J Am Chem Soc 122:11450
26. Alhambra C, Luque FJ, Orozco M (1995) J Phys Chem 99:3084
27. Ribas J, Cubero E, Luque FJ, Orozco M (2002) J Org Chem 67:7057
28. Hirota M, Sakaibara K, Suezawa H, Yuzuri T, Ankai E, Nishio MJ (2000) Phys Org Chem 13:620
29. Lindeman SV, Kosynkin D, Kochi JK (1998) J Am Chem Soc 120:13268
30. Hobza P, Selzle HL, Schalg EW (1996) J Phys Chem 100:18790
31. Cubero E, Orozco M, Hobza P, Luque FJ (1999) J Phys Chem 103:814
32. Hobza P, Havlas Z (2000) Chem Rev 100:4253
33. Tsuzuki S, Uchimaru T, Matsumura K, Mikami M, Tanabe K (2000) Chem Phys Lett 319:547
34. Hunter CA (1994) Chem Soc Rev 23:101
35. Bhattacharyya R, Samanta U, Chakrabarti P (2002) Protein Eng 15:91
36. Gurrath M, Müller G, Höltje H-D (1998) Perspect Drug Discov Des 12:135
37. Vedani A, Zbinden P, Snyder JP, Greenidge PA (1995) J Am Chem Soc 117:4987
38. Desiraju GR (1995) Angew Chem Int Ed Engl 34:2311
39. Shirakawa M, Fujita N, Shinkai S (2003) J Am Chem Soc 125:9902
40. Nierengarten J-F, Hahn U, Trabolsi A, Herschbach H, Cardinali F, Elhabiri M, Leize E, Van Dorsselaer A, Albrecht-Gary A-M (2006) Chem Eur J 12:3365
41. Kawase T, Tanaka K, Shiono N, Seirai Y, Oda M (2004) Angew Chem Int Ed 43:1722
42. Yamaguchi T, Ishii N, Tashiro K, Aida T (2003) J Am Chem Soc 125:13934
43. Kawase T, Kurata H (2006) Chem Rev 106:5250
44. Wang W, Pitonak M, Hobza, (2007) Chem Phys Chem 8:2107
45. Lee EC, Kim D, Jurecka P, Tarakeshwar P, Hobza P, Kim KS (2007) J Phys Chem A 111:3446
46. Spirko V, Engkvist O, Soldan P, Selzle HL, Schlag EW, Hobza P (1999) J Chem Phys 111:572
47. Müller-Dethlefs K, Hobza P (2000) Chem Rev 100:143
48. Hobza P, Spirko V, Selzle HL, Schlag EW (1998) J Phys Chem A 102:2501
49. Hobza P, Selzle HL, Schlag EW (1996) J Phys Chem 100:18790

50. Hobza P, Selzle HL, Schlag EW (1994) J Am Chem Soc 116:3500
51. Hobza P, Selzle HL, Schlag EW (1993) J Phys Chem 97:3937
52. Bader RFW (1991) Chem Rev 91:893
53. Bader RFW (1990) Atoms in molecules. A quantum theory. Clarendon, Oxford
54. Cheeseman JR, Carrol MT, Bader RFW (1998) Chem Phys Lett 143:450
55. Koch U, Popelier PLA (1995) J Phys Chem 99:9794
56. Cubero E, Orozco M, Luque FJ (1999) J Phys Chem A 103:315
57. Ahlrichs R, Bär M, Häser M, Horn H, Kölmel C (1989) Chem Phys Lett 162:165
58. Feyereisen MW, Fitzgerald G, Komornicki A (1993) Chem Phys Lett 208:359
59. Vahtras O, Almlof J, Feyereisen MW (1993) Chem Phys Lett 213:514
60. Frontera A, Quiñonero D, Garau C, Ballester P, Costa A, Deyà PM (2005) J Phys Chem A 109:4632
61. Quiñonero D, Garau C, Frontera A, Ballester P, Costa A, Deyà PM (2006) J Phys Chem A 110:5144
62. Shibasaki K, Fujii A, Mikami N, Tsuzuki S (2006) J Phys Chem A 110:4397
63. Janowski T, Pulay P (2007) Chem Phys Lett 447:27
64. Sinnokrot OM, Sherrill CD (2006) J Phys Chem A 110:10656
65. Boys SB, Bernardy F (1970) Mol Phys 19:553
66. http://www.AIM2000.de
67. Frontera A, Quiñonero D, Garau C, Ballester P, Costa A, Deyà PM, Pichierri F (2006) Chem Phys Lett 417:371
68. Luque FJ, Orozco M (1998) J Comput Chem 19:866
69. Hernández B, Orozco M, Luque FJ (1997) J Comput-Aided Mol Des 11:153
70. Luque FJ, Orozco M (1993) J Chem Soc, Perkin Trans 2:683
71. Quiñonero D, Frontera A, Garau C, Ballester P, Costa A, Deyà PM (2006) Chem Phys Chem 7:2487
72. Scrocco E, Tomasi J (1973) Top Curr Chem 42:95
73. Francl MM (1985) J Phys Chem 89:428
74. Luque FJ, Orozco M (1998) . Universitat de Barcelona, Barcelona (MIPp was computed using the MOPETE computer program)
75. Zhao Y, Tishchenko O, Truhlar DG (2005) J Phys Chem B 109:19046
76. Rodham D A, Suzuki S, Suenram RD, Lovas FJ, Dasgupta S, Goddard WA, Blake GA (1993) Nature 362:735
77. Mons M, Dimicoli I, Tardivel B, Piuzzi F, Brenner V, Millie P (2002) Phys Chem Chem Phys 4:571
78. Kim KS, Lee JY, Lee SJ, Ha T-K, Kim DH (1994) J Am Chem Soc 116:7399
79. Cubero E, Luque FJ, Orozco M (1998) Proc Natl Acad Sci USA 95:5976
80. Garau C, Frontera A, Quiñonero D, Ballester P, Costa A, Deyà PM (2003) ChemPhysChem 4:1344
81. Garau C, Frontera A, Quiñonero D, Ballester P, Costa A, Deyà PM (2004) J Phys Chem A 108:9423
82. Alkorta I, Quiñonero D, Garau C, Frontera A, Elguero J, Deyà PM (2007) J Phys Chem A 111:3137
83. Espinosa E, Alkorta I, Elguero J, Molins E (2002) J Chem Phys 117:5529
84. Alkorta I, Barrios L, Rozas I, Elguero J (2000) Theochem 496:131
85. Knop O, Boyd RJ (1988) J Am Chem Soc 110:7299
86. Kryger G, Silman I, Sussman JL (1999) Struct Fold Des 7:297
87. Istvan ES, Deisenhofer J (2001) Science 292:1160
88. Burkhard P, Dominici P, Borri-Voltattorni C, Jansonius JN, Malashkevich VN (2001) Nat Struct Biol 8:963